Latin American Journal of Solids and Structures
www.lajss.org

Nonlinear Vibrations of Cantilever Timoshenko Beams: A Homotopy Analysis

Abstract

This study analyzes the fourth-order nonlinear free vibration of a Timoshenko beam. We discretize the governing differential equation by Galerkin's procedure and then apply the homotopy analysis method (HAM) to the obtained ordinary differential equation of the generalized coordinate. We derive novel analytical solutions for the nonlinear natural frequency and displacement to investigate the effects of rotary inertia, shear deformation, pre-tensile loads and slenderness ratios on the beam. In comparison to results achieved by perturbation techniques, this study demonstrates that a first-order approximation of HAM leads to highly accurate solutions, valid for a wide range of amplitude vibrations, of a high-order strongly nonlinear problem.

Keywords

strongly nonlinear vibration, homotopy analysis method, Galerkin method, Timoshenko beam, nonlinear natural frequency

Shahram Shahlaei-Far
Airton Nabarrete *
José Manoel Balthazar

Instituto Tecnológico de Aeronáutica, Praça Marechal Eduardo Gomes 50, São José dos Campos, SP, 12228-900, Brazil

*Corresponding author: nabarret@ita.br

http://dx.doi.org/10.1590/1679-78252766

Received 05.01.2016
Accepted 14.04.2016
Available online 21.04.2016

1 INTRODUCTION

This study presents a closed-form analytical solution for a thick beam considering the Timoshenko formulation for various values of the relevant design parameters applying the homotopy analysis method (HAM), introduced by Liao (1998; 2003; 2004; 2007; 2009). Making no use of small parameters it allows us to consider the general nonlinear system for small as well as large amplitude vibrations. Thus it overcomes the requirement for perturbation techniques, such as the multiple scales method, to model the problem as a weakly nonlinear system involving perturbation quantities. To ensure accurate results the partial differential equation is first discretized by the Galerkin procedure before HAM is applied to the obtained nonlinear ordinary differential equation.

Previously, Ramezani et al. (2006) provided a second-order perturbation solution for a doubly clamped Timoshenko microbeam using the multiple scales method. Moeenfard et al. (2011) also analyzed this problem by applying the homotopy perturbation method. Foda (1999) analyzed the same problem in macro-scale with perturbation methods considering the pinned boundary condi-

tion. A comparison to results from Ramezani et al. (2006) for the doubly clamped case shows the formidable accuracy of HAM. Furthermore, a parametric study discusses the effects of applied tensile loads and slenderness ratios on the large amplitude vibration of the cantilever Timoshenko beam. The analysis also addresses the effects of rotary inertia and shear deformation on the nonlinear natural frequency.

The homotopy analysis method is a nonperturbative analytical technique for obtaining series solutions to nonlinear equations. Its freedom to choose different base functions to approximate a nonlinear problem and its ability to control the convergence of the solution series have been very advantageous in solving highly nonlinear problems in science and engineering (Hoseini et al., 2008; Hoshyar et al., 2015; Mastroberardino, 2011; Mehrizi et al., 2012; Mustafa et al., 2012; Pirbodaghi and Hoseini, 2009; Pirbodaghi et al., 2009; Qian et al., 2011; Ray and Sahoo, 2015; Sedighi et al., 2012; Wen and Cao, 2007; Wu et al., 2012).

2 GOVERNING DIFFERENTIAL EQUATION

The nonlinear free vibration of a thick beam considering the Timoshenko formulation for the midplane stretching and the effects of rotary inertia and shear deformation was first reviewed by Ramezani et al. (2006). In that article, a full description of the problem was presented in which the governing equation was derived as

$$EI\frac{\partial^4 w}{\partial x^4}+m\frac{\partial^2 w}{\partial t^2}-\left(mr^2+\frac{mEI}{\kappa AG}\right)\frac{\partial^4 w}{\partial x^2\partial t^2}+\frac{m^2r^2}{\kappa AG}\frac{\partial^4 w}{\partial t^4}- N\left[\frac{\partial^2 w}{\partial x^2}-\frac{EI}{\kappa AG}\frac{\partial^4 w}{\partial x^4}+\frac{mr^2}{\kappa AG}\frac{\partial^4 w}{\partial x^2\partial t^2}\right]=0 \tag{1}$$

where w is the transverse displacement, x is the axial coordinate of the beam and t is the time. As constant terms, E is the modulus of elasticity, G is the shear modulus, A is the cross-section area, I is the second moment of area of the cross section with respect to the bending axis, r is the radius of gyration of the beam cross section given by $r^2 = I/A$, m is mass per unit length and κ is the shear correction factor that depends only on the geometric properties of the cross section of the beam.

The last bracketed terms in Eq. 1 represent the nonlinearity due to large amplitudes caused by the axial force N, which is given by

$$N = N_0 + \frac{EA}{2L}\int_0^L\left(\frac{\partial w}{\partial x}\right)^2 dx \tag{2}$$

where N_0 is the pre-tensile load and L is the length of the beam.

For convenience, we take the nondimensional quantities

$$\hat{x}=\frac{x}{L},\quad \hat{w}=\frac{w}{L}\quad\text{and}\quad \hat{t}=\frac{t}{T},\quad\text{with}\quad T=\frac{1}{\beta^2}\sqrt{\frac{m}{EI}} \tag{3}$$

where β is the numerical solution for $\cos\beta L \cosh\beta L = -1$ of a corresponding Euler-Bernoulli beam (Meirovitch, 2001).

Considering $\beta L = \hat{\beta}$, Eqs. (1) and (2) are rewritten in nondimensional form

$$\frac{\partial^4 \hat{w}}{\partial \hat{x}^4} - \hat{\beta}^4 \left(\frac{r}{L}\right)^2 \left(1 + \frac{E}{\kappa G}\right) \frac{\partial^4 \hat{w}}{\partial \hat{x}^2 \partial \hat{t}^2} + \hat{\beta}^8 \left(\frac{r}{L}\right)^4 \left(\frac{E}{\kappa G}\right) \frac{\partial^4 \hat{w}}{\partial \hat{t}^4} + \hat{\beta}^4 \frac{\partial^2 \hat{w}}{\partial \hat{t}^2} + \frac{N}{EA} \left(\frac{L}{r}\right)^2 \left(\left(\frac{r}{L}\right)^2 \left(\frac{E}{\kappa G}\right) \frac{\partial^4 \hat{w}}{\partial \hat{x}^4} - \hat{\beta}^4 \left(\frac{r}{L}\right)^4 \left(\frac{E}{\kappa G}\right) \frac{\partial^4 \hat{w}}{\partial \hat{x}^2 \partial \hat{t}^2} - \frac{\partial^2 \hat{w}}{\partial \hat{x}^2} \right) = 0 \tag{4}$$

$$N = N_0 + \frac{EA}{2} \int_0^1 \left(\frac{\partial \hat{w}}{\partial \hat{x}}\right)^2 d\hat{x} \tag{5}$$

The boundary conditions for a cantilever beam formulated in this research are

$$\begin{aligned} \hat{w} = 0 \ , \quad \frac{\partial \hat{w}}{\partial \hat{x}} = 0 \quad \text{at} \quad \hat{x} = 0 \\ \frac{\partial^2 \hat{w}}{\partial \hat{x}^2} = 0 \ , \quad \frac{\partial^3 \hat{w}}{\partial \hat{x}^3} = 0 \quad \text{at} \quad \hat{x} = 1 \end{aligned} \tag{6}$$

Hereafter the caret on all the variables is dropped for convenience.

The nondimensional transverse displacement is here approximated as $w(x,t) = \Theta(x) W(t)$ where $\Theta(x)$ is the normalized mode shape of the corresponding cantilever Euler-Bernoulli beam and $W(t)$ the corresponding time-dependent generalized coordinate.

The average over the space variable is applied to reduce Eq. (4) to an ordinary differential equation. Multiplying Eq. (4) by $\Theta(x)$ and integrating it over the interval of $[0,1]$, the governing nonlinear differential equation is derived as

$$\dddot{W} + (\alpha_1 + \alpha_2 W^2)\ddot{W} + \alpha_3 W + \alpha_4 W^3 = 0 \tag{7}$$

where the dot represents differentiation with respect to time t and the parameters α_j for $j = 1,2,3,4$ are given by

$$\begin{aligned} \alpha_1 &= \frac{\rho^2}{{\beta_1}^4} \left[\rho^2 \frac{\kappa G}{E} - \delta_1 \left(1 + \frac{\kappa G}{E} + \frac{N_0}{EA}\right) \right], & \alpha_2 &= -\frac{\rho^2}{2{\beta_1}^4} \delta_3 \delta_1, \\ \alpha_3 &= \frac{\rho^4}{{\beta_1}^8} \left[\delta_2 \left(\frac{\kappa G}{E} + \frac{N_0}{EA}\right) - \rho^2 \delta_1 \left(\frac{\kappa G}{E}\right)\left(\frac{N_0}{EA}\right) \right], & \alpha_4 &= \frac{\rho^4}{2{\beta_1}^8} \left(\delta_3 \delta_2 - \rho^2 \delta_3 \delta_1 \left(\frac{\kappa G}{E}\right) \right) \end{aligned} \tag{8}$$

where $\rho = L/r$ and δ_i for $i = 1,2,3,4$ are the integration results denoted by

$$\delta_1 = \frac{\int_0^1 \Theta'' \Theta \, dx}{\int_0^1 \Theta^2 \, dx}, \qquad \delta_2 = \frac{\int_0^1 \Theta'''' \Theta \, dx}{\int_0^1 \Theta^2 \, dx}, \quad \delta_3 = \int_0^1 \left(\Theta'\right)^2 dx \tag{9}$$

where the prime denotes differentiation with respect to the spatial variable x.

Let $\tau = \omega t$ denote a new time scale. Under the transformation

$$\tau = \omega t \ , \quad \mathrm{V}(\tau) = W(t) \tag{10}$$

Eq. (7) becomes

$$\omega^4 \frac{d^4 V(\tau)}{d\tau^4} + \omega^2 \left[\alpha_1 + \alpha_2 V^2(\tau)\right] \frac{d^2 V(\tau)}{d\tau^2} + \alpha_3 V(\tau) + \alpha_4 V^3(\tau) = 0 \tag{11}$$

The nonlinear ordinary differential equation is subject to the following initial conditions

$$V(0) = \frac{W_{\max}}{L}, \qquad \frac{dV(0)}{d\tau} = \frac{d^2 V(0)}{d\tau^2} = \frac{d^3 V(0)}{d\tau^3} = 0 \tag{12}$$

where $W_{\max}$ is the amplitude at the free end of the beam.

3 HOMOTOPY ANALYSIS METHOD

The homotopy analysis method is an analytical technique for solving general nonlinear differential equations. It transforms a nonlinear differential equation into an infinite number of linear differential equations embedding an auxiliary parameter $q \in [0,1]$. As q increases from 0 to 1, the solution varies from the initial guess to the exact solution (Liao, 2003).

Free oscillation without damping is a periodic motion and can be expressed by the following set of base functions

$$\{\cos(m\tau) \mid m = 1,2,3,\ldots\} \tag{13}$$

such that the general solution is given as

$$V(\tau) = \sum_{i=1}^{\infty} g_i \cos(m\tau) \tag{14}$$

where g_i are coefficients to be determined. We choose the initial guess

$$V_0(\tau) = \frac{9}{8} D \cos(\tau) - \frac{1}{8} D \cos(3\tau) \quad \text{with} \quad D = \frac{W_{max}}{L} = \frac{W_{max}}{h} \frac{s}{\rho}, \quad s \rangle \ \frac{h}{r} \approx 3.46416 \tag{15}$$

where h is the thickness of the beam. The initial guess satisfies the initial conditions in Eq. (12).

According to Eq. (11) we define the nonlinear operator to be

$$\boldsymbol{\mathcal{N}}\left[\phi(\tau;q),\omega\right] = \omega^4 \frac{\partial^4\phi(\tau;q)}{\partial\tau^4} + \omega^2[\alpha_1 + \alpha_2\phi^2(\tau;q)]\frac{\partial^2\phi(\tau;q)}{\partial\tau^2} + \alpha_3\phi(\tau;q) + \alpha_4\phi^3(\tau;q) \tag{16}$$

where q is an embedding parameter and $\phi(\tau;q)$ is a function of τ and q. To ensure the *rule of solution expression* given by Eq. (14) we choose the linear operator to be

$$\boldsymbol{\mathcal{L}}\left[\phi(\tau;q)\right] = \omega^4\left(\frac{\partial^4\phi(\tau;q)}{\partial\tau^4} + \frac{\partial^2\phi(\tau;q)}{\partial\tau^2}\right) \tag{17}$$

with the property

$$\boldsymbol{\mathcal{L}}\left[C_1 + C_2\tau + C_3\cos(\tau) + C_4\sin(\tau)\right] = 0 \tag{18}$$

where C_1, C_2, C_3 and C_4 are constants of integration.

Now, we can construct a homotopy

$$\mathrm{H}(\phi(\tau;q);V_0(\tau),H(\tau),c_0,q) = (1-q)\boldsymbol{\mathcal{L}}\left[\phi(\tau;q) - V_0(\tau)\right] - qc_0H(\tau)\boldsymbol{\mathcal{N}}\left[\phi(\tau;q),\omega\right] \tag{19}$$

where $c_0 \neq 0$ is the convergence-control parameter and $H(\tau)$ a nonzero auxiliary function. Enforcing the homotopy in Eq. (19) to be zero, i.e. $\mathrm{H}(\phi(\tau;q);V_0(\tau),H(\tau),c_0,q) = 0$, we obtain the zero-order deformation equation

$$(1-q)\boldsymbol{\mathcal{L}}\left[\phi(\tau;q) - V_0(\tau)\right] = qc_0H(\tau)\boldsymbol{\mathcal{N}}\left[\phi(\tau;q),\omega\right] \tag{20}$$

In Eq. (20), for $q = 0$ and $q = 1$ we have, respectively,

$$\phi(\tau;0) = V_0(\tau) \quad \text{and} \quad \phi(\tau;1) = V(\tau) \tag{21}$$

Thus, the function $\phi(\tau;q)$ varies from the initial guess $V_0(\tau)$ to the desired solution as q varies from 0 to 1. The Taylor expansions of $\phi(\tau;q)$ with respect to q is

$$\phi(\tau;q) = V_0(\tau) + \sum_{m=1}^{\infty} V_m(\tau)q^m \tag{22}$$

where

$$V_m(\tau) = \frac{1}{m!}\frac{\partial^m\phi(\tau;q)}{\partial q^m}\Big|_{q=0} \tag{23}$$

Choosing properly the linear operator, the initial guess, the auxiliary function $H(\tau)$ and the convergence-control parameter c_0, the series in Eq. (22) converges when $q = 1$, such that

$$V(\tau) = V_0(\tau) + \sum_{m=1}^{\infty} V_m(\tau) \tag{24}$$

Differentiating the zero-order equation (20) with respect to q and setting $q = 0$, the first-order deformation equation is obtained as

$$\boldsymbol{\mathcal{L}}\left[V_1(\tau)\right] = c_0 H(\tau)\boldsymbol{\mathcal{N}}\left[V_0(\tau),\omega\right] \tag{25}$$

subject to the initial conditions

$$V_1(0) = \frac{dV_1(0)}{d\tau} = 0 \tag{26}$$

For the nonzero auxiliary function $H(\tau)$ to obey the *rule of solution expression* and the *rule of coefficient ergodicity*, we choose it to be

$$H(\tau) = \cos(2k\tau) \tag{27}$$

where k is an integer. It can be determined uniquely as $H(\tau) = 1$.

As a result, Eq. (25) becomes

$$\begin{aligned}\omega^4\left(\frac{d^4V_1(\tau)}{d\tau^4} + \frac{d^2V_1(\tau)}{d\tau^2}\right) &= c_0\left[\omega^4\frac{d^4V_0(\tau)}{d\tau^4} + \omega^2(\alpha_1 + \alpha_2 V_0^2(\tau))\frac{d^2V_0(\tau)}{d\tau^2} + \alpha_3 V_0(\tau) + \alpha_4 {V_0}^3(\tau)\right] \\ &= c_0[b_{1,0}(V_0,\omega)\cos(\tau) + b_{1,1}(V_0,\omega)\cos(3\tau) + b_{1,2}(V_0,\omega)\cos(5\tau) + \\ &\quad b_{1,3}(V_0,\omega)\cos(7\tau) + b_{1,4}(V_0,\omega)\cos(9\tau)]\end{aligned} \tag{28}$$

where the coefficients $b_{1,i}(V_0,\omega)$, $i = 0,1,2,3,4$ are obtained as

$$\begin{aligned} b_{1,0} &= \frac{9}{8}\omega^4 D - \omega^2\left(\frac{9}{8}\alpha_1 D + \frac{819}{1024}\alpha_2 D^3\right) + \frac{9}{8}\alpha_3 D + \frac{999}{1024}\alpha_4 D^3 \\ b_{1,1} &= -\frac{81}{8}\omega^4 D - \omega^2\left(\frac{9}{8}\alpha_1 D + \frac{135}{256}\alpha_2 D^3\right) - \frac{1}{8}\alpha_3 D + \frac{15}{128}\alpha_4 D^3 \\ b_{1,2} &= \frac{45}{128}\omega^2\alpha_2 D^3 - \frac{27}{256}\alpha_4 D^3 \\ b_{1,3} &= -\frac{171}{2048}\omega^2\alpha_2 D^3 + \frac{27}{2048}\alpha_4 D^3 \\ b_{1,4} &= \frac{9}{2048}\omega^2\alpha_2 D^3 - \frac{1}{2048}\alpha_4 D^3 \end{aligned} \tag{29}$$

According to the property of the linear operator, if the term $\cos(\tau)$ exists on the right side of Eq. (28), the secular term $\tau\sin(\tau)$ will appear in the final solution. Thus, to obey the *rule of solution expression*, the coefficient $b_{1,0}$ has to be equal to zero. Solving the algebraic equation for the nonlinear natural frequency, it is obtained as

$$\omega_{nl} = \left(\left(\frac{91}{256}\alpha_4 D^2 + \frac{1}{2}\alpha_1\right) - F\right)^{\frac{1}{2}} \tag{30}$$

with

$$F = \left(\left(\frac{91}{256}\alpha_4 D^2 + \frac{1}{2}\alpha_1 \right)^2 - \left(\alpha_3 + \frac{111}{128}\alpha_4 D^2 \right) \right)^{\frac{1}{2}} \tag{31}$$

There are two sinusoidal modes of different frequencies. For our purposes we consider the lower fundamental frequency which is associated with bending deformation.

Finally, solving Eq. (28) for the displacement of the beam, the general solution of Eqs. (11) and (12) is achieved as

$$\begin{aligned} V_1(\tau) &= V_1^*(\tau) + C_1 + C_2\tau + C_3\cos(\tau) + C_4\sin(\tau) \\ &= \frac{c_0}{\omega_{nl}^4}\sum_{n=1}^{4}\frac{b_{1,n}}{(2n+1)^2((2n+1)^2-1)}\cos((2n+1)\tau) + C_3\cos(\tau) \\ &= \frac{c_0}{\omega_{nl}^4}\left(\frac{b_{1,1}}{72}(\cos(3\tau)-\cos(\tau)) + \frac{b_{1,2}}{600}(\cos(5\tau)-\cos(\tau)) \right. \\ &\quad \left. + \frac{b_{1,3}}{2352}(\cos(7\tau)-\cos(\tau)) + \frac{b_{1,4}}{6480}(\cos(9\tau)-\cos(\tau)) \right) \end{aligned} \tag{32}$$

where $V_1^*(\tau)$ is the special solution, $C_1 = C_2 = C_4 = 0$ to comply with the *rule of solution expression* and C_3 is obtained from the initial conditions given in Eq. (24).

Thus, with Eq. (24) the first-order approximation of $W(t)$ becomes

$$\begin{aligned} W(t) &= V(\tau) \approx V_0(\tau) + V_1(\tau) \\ &= \left(\frac{9}{8}D - \frac{c_0}{\omega_{nl}^4}\left(\frac{b_{1,1}}{72} + \frac{b_{1,2}}{600} + \frac{b_{1,3}}{2352} + \frac{b_{1,4}}{6480} \right) \right)\cos(\omega_{nl}t) - \left(\frac{1}{8}D - \frac{c_0}{\omega_{nl}^4}\frac{b_{1,1}}{72} \right)\cos(3\omega_{nl}t) \\ &\quad + \frac{c_0}{\omega_{nl}^4}\left(\frac{b_{1,2}}{600}\cos(5\omega_{nl}t) + \frac{b_{1,3}}{2352}\cos(7\omega_{nl}t) + \frac{b_{1,4}}{6480}\cos(9\omega_{nl}t) \right) \end{aligned} \tag{33}$$

4 RESULTS

The effects of rotary inertia and shear deformation as well as vibration amplitude for various design parameters on the nonlinear natural frequency of thick and short beams for the clamped-free boundary condition are discussed in this section. The accuracy of a first-order approximation of the homotopy analysis method is confirmed by comparison with results obtained from Ramezani et al. (2006) for clamped-clamped microbeams. The geometric and material properties of the Timoshenko beam in consideration are given in Table 1. For purposes of comparison the natural linear frequency ω_l of the Euler-Bernoulli beam theory, given by $\omega_l^2 = \frac{1}{\beta^4}\left(\delta_2 - \frac{N_0}{EA}\left(\frac{L}{r}\right)^2 \delta_1 \right)$, is used.

Property	E	G	ρ	A	κ
Value	169 GPa	66 GPa	2330 kg/m^3	90 μm^2	5/6

Table 1: Geometric and material properties of the Timoshenko beam.

In Figure 1 we observe that a first-order approximation of the HAM provides excellent agreement with results achieved by Ramezani et al. (2006) for doubly clamped microbeams. Three slenderness ratios have been considered ranging from thick $\left(L/r = 20\right)$ to slender beams $\left(L/r = 100\right)$. For the calculation, the first normalized mode of vibration $\Theta(x)$ and the value for $\beta = \beta_1$ have been adequately adjusted with respect to the boundary condition.

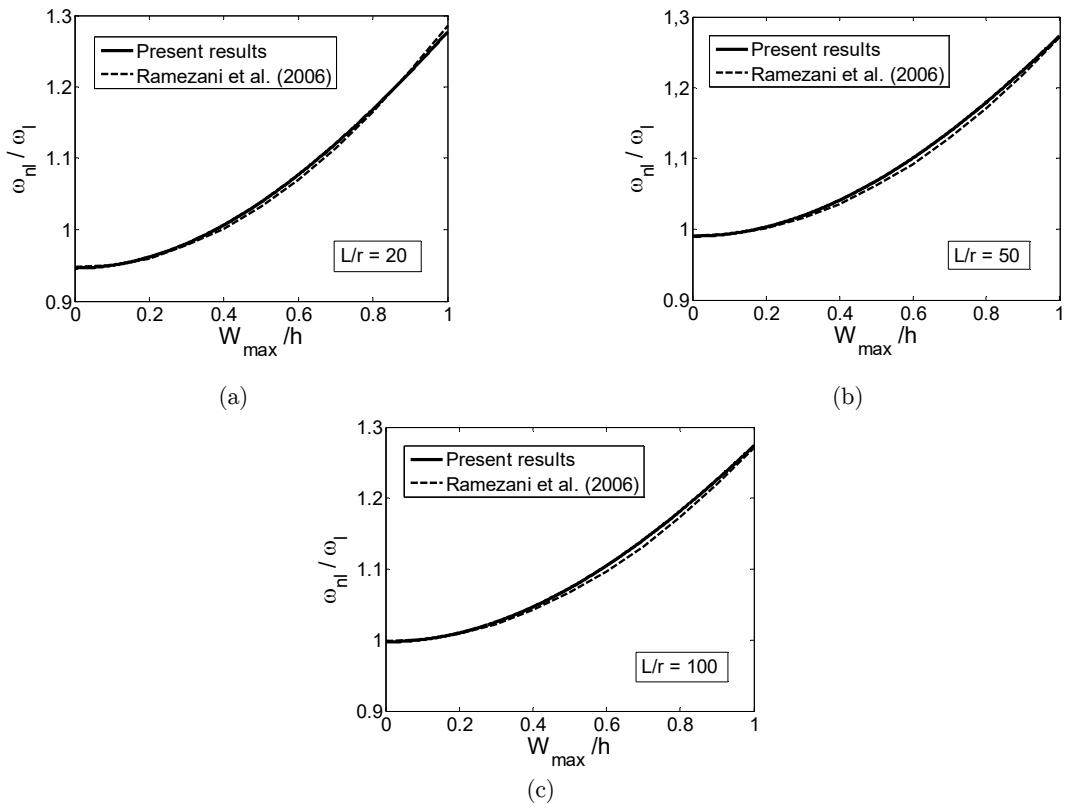

Figure 1: Nonlinear frequency of clamped-clamped beam for different slenderness ratios.

The rest of our discussion deals with cantilever Timoshenko beams. Applying HAM to a nonlinear problem results in a family of solution series which depend on the convergence-control parameter. The optimal value is obtained by minimizing the square residual error of the governing equation for a given order of approximation. For a first-order approximation, Figure 2 presents the time-domain response of the nonlinear system in accurate agreement with numerical results. Considering $L/r = 10, 20, 30$ the length-to-thickness ratios are $L/h \approx 2.8867, 5.7734, 8.6601$, respectively. The stretching effect occurring at the beam's centerline causes the nonlinear frequency to increase

considerably (over 70%) with the increase of the initial deflection $W_{\max}/h$ as seen in Figure 3. At small deflections, there are no significant discrepancies between the linear and nonlinear model which suggests that for weak nonlinearity linear models would give sufficiently reasonable estimates.

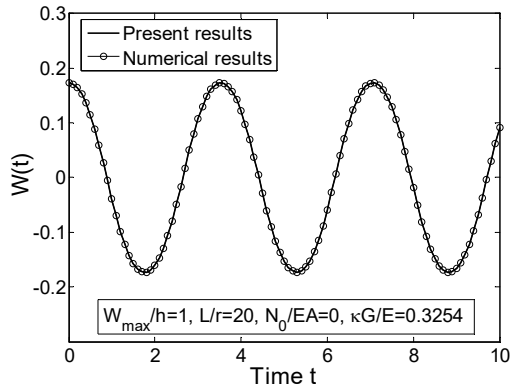

Figure 2: Time response of clamped-free beam for $c_0 = 0.0048$.

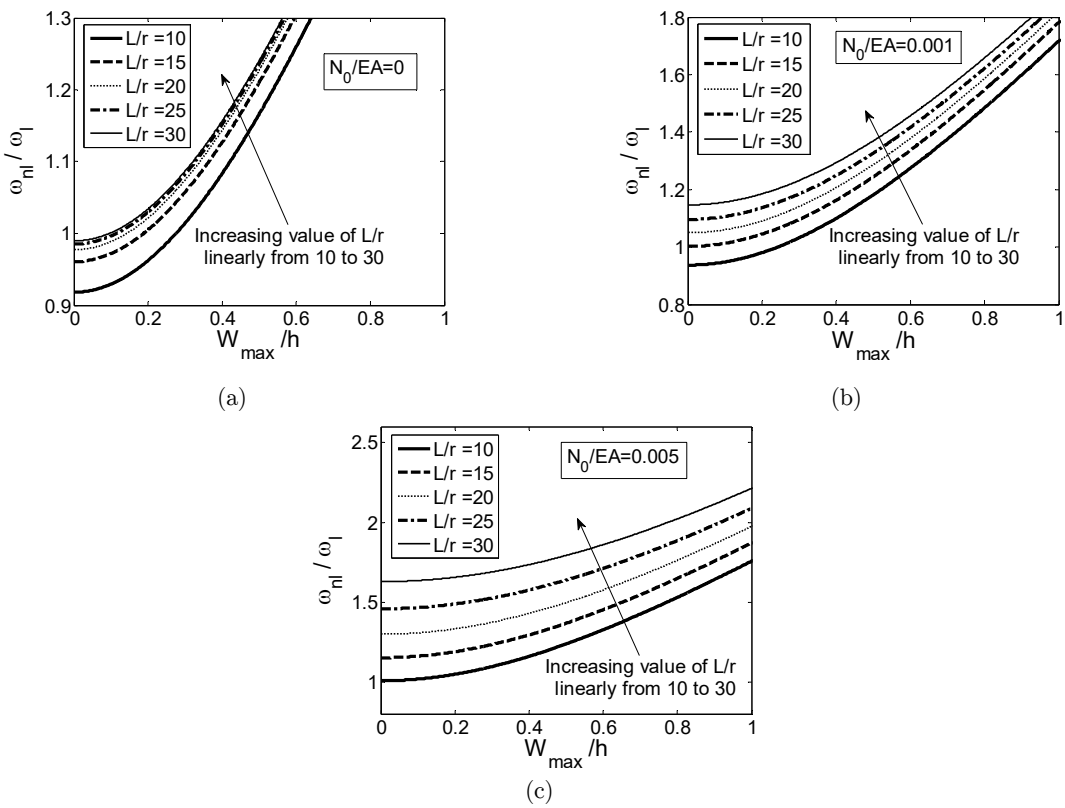

Figure 3: Nonlinear frequency of clamped-free beam for varying slenderness ratios.

Moreover, Figure 3 depicts the influence of the slenderness ratio on the nonlinear frequency for different values of the pre-tensile load. At small values of $W_{\max}/h$, increasing L/r linearly, the nonlinear frequency increases considerably for all values of the pre-tensile load, whereby the nonlinearity effect for lower values of L/r is more substantial. On the other hand, for large values of $W_{\max}/h$, the difference between the nonlinear frequencies corresponding to different slenderness ratios becomes smaller.

For given slenderness ratios the influence of varying pre-tensile loads is demonstrated in Figure 4. The nonlinear frequency of the beam is augmented when linearly increasing pre-tensile axial loads are applied having greater impact at small values of $W_{\max}/h$.

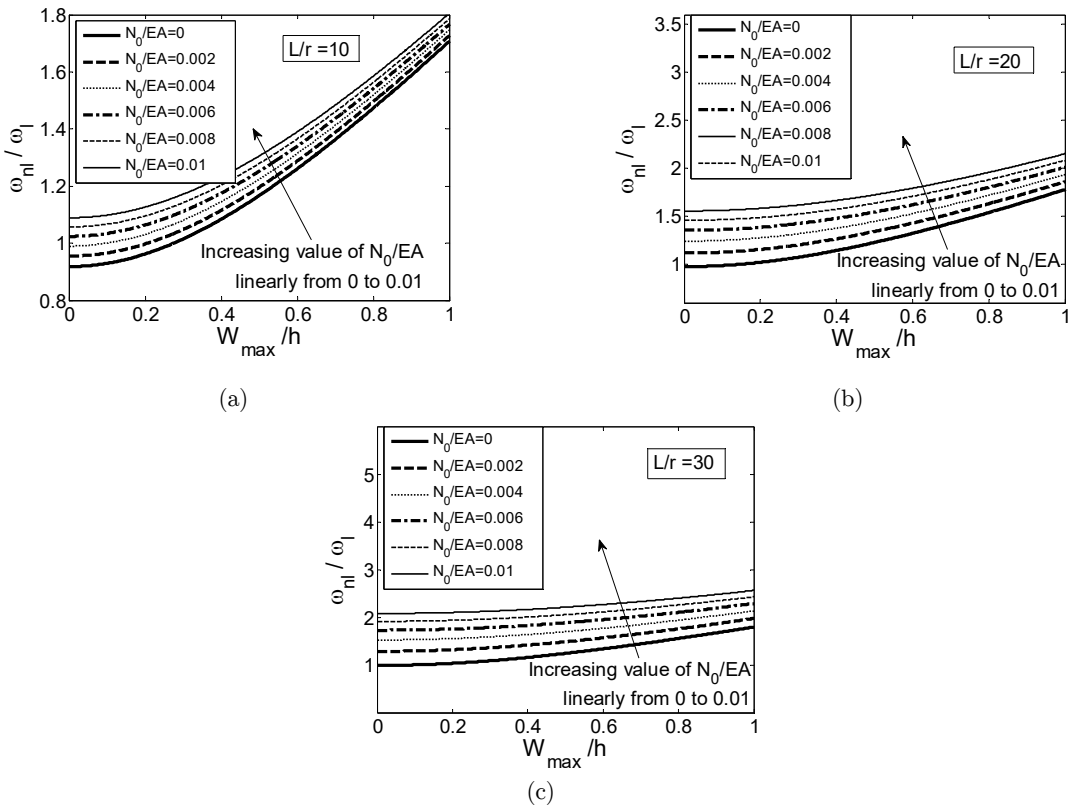

Figure 4: Nonlinear frequency of clamped-free beam for varying pre-tensile loads.

In Figures 5 and 6 the effects of rotary inertia and shear deformation on the large amplitude vibration are depicted, where the nonlinear frequency is plotted against $\kappa G/E$ and L/r, respectively. In both cases, the nonlinear frequency converges to a definite value when $\kappa G/E$ and L/r are being increased, respectively. Thus for slender beams the effects of rotary inertia and shear deformation are negligible as expected. On the other hand, for any thick beam analysis they must be included.

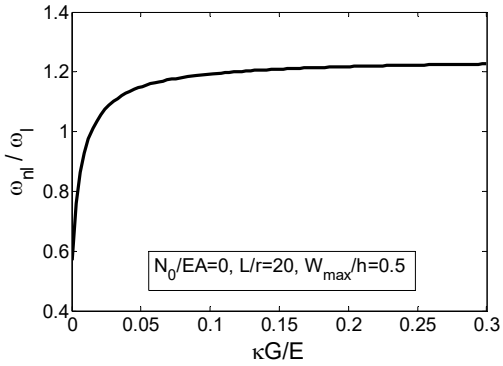

Figure 5: Influence of rotary inertia on nonlinear frequency of clamped-free beam.

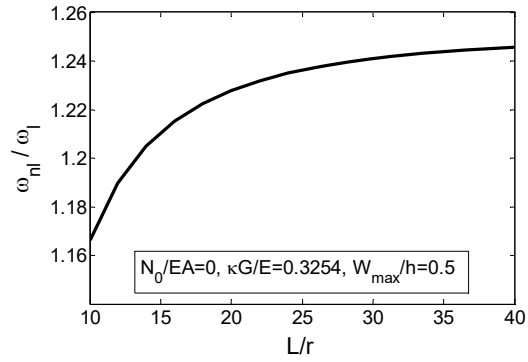

Figure 6: Influence of shear deformation on nonlinear frequency of clamped-free beam.

5 CONCLUSIONS

The present study analyzed free nonlinear vibrations of Timoshenko beams by means of the homotopy analysis method to yield straightforward closed-form expressions for the nonlinear natural frequency and the generalized coordinate corresponding to the first spatial mode. The efficiency and accuracy of the method was demonstrated by a comparison between solutions obtained by HAM and perturbation methods for the clamped-clamped boundary condition.

In the case of cantilever Timoshenko beams, we investigated the effects of rotary inertia and shear deformation as well as the influence of design parameters such as the slenderness ratio and pre-tensile loads on the nonlinear natural frequency. Higher natural frequencies are observed for the nonlinear model when pre-tensile loads or slenderness ratios are increased. By augmenting the effect of shear deformation and rotary inertia, respectively, the nonlinear natural frequency of the beam rises significantly and converges to a definite value. Moreover, it is shown that the time response of the nonlinear system agrees accurately with numerical results.

Unlike perturbation methods, HAM is valid for a wide range of parameters and vibration amplitudes as it does not require small parameters for its analysis and the study shows that a first-order homotopy approximation efficiently obtains accurate analytical results for a high-order strongly nonlinear problem.

References

Foda, M.A., (1999). Influence of shear deformation and rotary inertia on nonlinear free vibration of a beam with pinned ends. Computers & Structures 71:663–670.

Hoseini, S.H., Pirbodaghi, T., Asghari, M., Farrahi, G.H., Ahmadian, M.T., (2008). Nonlinear free vibration of conservative oscillators with inertia and static type cubic nonlinearities using homotopy analysis method. Journal of Sound and Vibration 316:263–273.

Hoshyar, H.A., Ganji, D.D., Borran, A.R., Falahati, M., (2015). Flow behavior of unsteady incompressible Newtonian fluid between two parallel plates via homotopy analysis method. Latin American Journal of Solids and Structures 12:1859–1869.

Liao, S.J. (2003). Beyond perturbation: Introduction to homotopy analysis method, Chapman&Hall/CRC Press (Boca Raton).

Liao, S.J., (2004). On the homotopy analysis method for nonlinear problems. Applied Mathematics and Computation 147:499–513.

Liao, S.J., (2009). Notes on the homotopy analysis method: Some definitions and theorems. Communications in Nonlinear Science and Numerical Simulation 14:983–997.

Liao, S.J., Cheung, A.T., (1998). Application of homotopy analysis method in nonlinear oscillations. ASME Journal of Applied Mechanics 65:914–922.

Liao, S.J., Tan, Y., (2007). A general approach to obtain series solutions of nonlinear differential equations. Studies in Applied Mathematics 119:297–355.

Mastroberardino, A., (2011). Homotopy analysis method applied to electrohydrodynamic flow. Communications in Nonlinear Science and Numerical Simulation 16:2730–2736.

Mehrizi, A.A., Vazifeshenas, Y., Domairry, G., (2012). New analysis of natural convection boundary layer flow on a horizontal plate with variable wall temperature. Journal of Theoretical and Applied Mechanics 50(4):1001–1010.

Meirovitch, L., (2001). Fundamentals of Vibrations, McGraw-Hill (New York).

Moeenfard, H., Mojahedi, M., Ahmadian, M.T., (2011). A homotopy perturbation analysis of nonlinear free vibration of Timoshenko microbeams. Journal of Mechanical Science and Technology 35(3):557–565.

Mustafa, M., Hayat, T., Hendi, A.A., (2012). Influence of melting heat transfer in the stagnation-point flow of a Jeffrey fluid in the presence of viscous dissipation. ASME Journal of Applied Mechanics 79(2):4501–4505.

Pirbodaghi, T., Ahmadian, M.T., Fesanghary, M., (2009). On the homotopy analysis method for non-linear vibration of beams. Mechanics Research Communications 36(2):143–148.

Pirbodaghi, T., Hoseini, S., (2009). Nonlinear free vibration of a symmetrically conservative two-mass system with cubic nonlinearity. ASME Journal of Computational and Nonlinear Dynamics 5(1):1006–1011.

Qian, Y. H., Lai, S. K., Zhang, W., Xiang, Y., (2011), Study on asymptotic analytical solutions using HAM for strongly nonlinear vibrations of a restrained cantilever beam with an intermediate lumped mass. Numerical Algorithm 58:293–314.

Ramezani, A., Alasty, A., Akbari, J., (2006). Effects of rotary inertia and shear deformation on nonlinear free vibration of microbeams. ASME Journal of Vibration and Acoustics 128(5):611–615.

Ray, S.S., Sahoo, S., (2015). Traveling wave solutions to Riesz time-fractional Camassa–Holm equation in modeling for shallow-water waves. ASME Journal of Computational and Nonlinear Dynamics 10(6):1026–1030.

Sedighi, H.M., Shirazi, K.H., Zare, J., (2012). An analytic solution of transversal oscillation of quintic non-linear beam with homotopy analysis method. International Journal of Non-linear Mechanics 47:777–784.

Wen, J., Cao, Z., (2007). Sub-harmonic resonances of nonlinear oscillations with parametric excitation by means of the homotopy analysis method. Physics Letters A 371:427–431.

Wu, R., Wang, J., Du, J., Hu, Y., Hu, H., (2012). Solutions of nonlinear thickness-shear vibrations of an infinite isotropic plate with the homotopy analysis method. Numerical Algorithm 59:213–226.